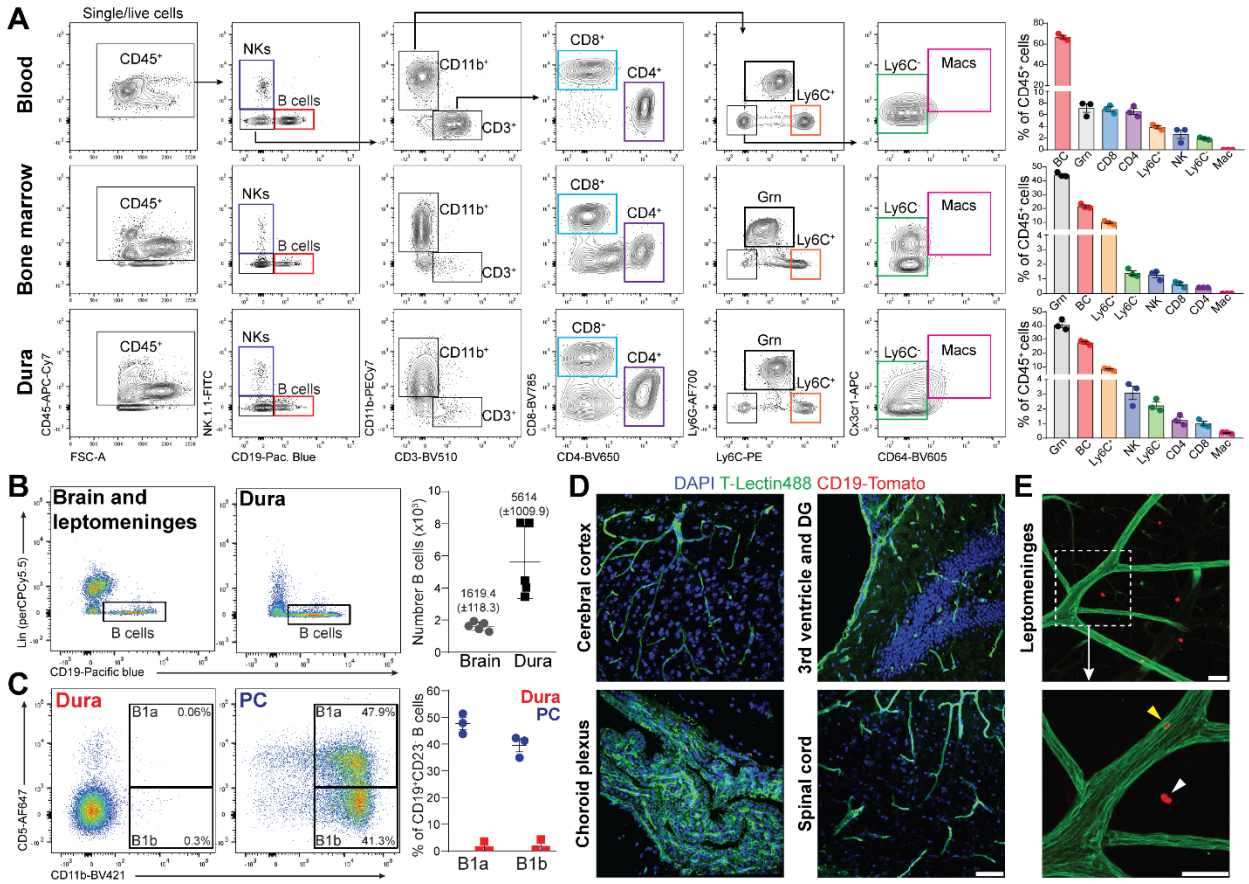

Fig. S1. Major immune populations in mouse dura mater. (A) Flow cytometry analysis of blood, BM and dura immune cells. Left panels, representative flow cytometry plots of NK cells ($CD45^+NK1.1^+$), B cells ($CD45^+CD19^+$), CD4 T cells ($CD45^+NK1.1^-CD19^-CD11b^-CD3^+CD4^+$), CD8 T cells ($CD45^+NK1.1^-CD19^-CD11b^-CD3^+CD8^+$), Granulocytes ($CD45^+NK1.1^-CD19^-CD11b^+CD3^-Ly6G^+Ly6C^{int}$), $Ly6C^+$ monocytes ($CD45^+NK1.1^-CD19^-CD11b^+CD3^-Ly6G^-Ly6C^+$), $Ly6C^-$ monocytes ($CD45^+NK1.1^-CD19^-CD11b^+CD3^-Ly6G^-Ly6C^-CD64^-$) and Macrophages ($CD45^+NK1.1^-CD19^-CD11b^+CD3^-Ly6G^-Ly6C^-CD64^+Cx3CR1^+$). Right panel, frequency of the immune populations identified in blood, BM and dura, out of total $CD45^+$ (n=3 mice; data generated from a single experiment). **(B)** Flow cytometry staining for B cells in brain and dura. The dot-plot reports the absolute number of B cells (n=5 mice; data generated from two independent experiment). **(C)** Flow cytometry staining for B1a and B1b cells in dura and peritoneal cavity (PC). The dot-plot reports the percentage of B1a and B1b cells within the $CD19^+CD23^-$ population (n=3 mice; data generated from a single experiment). **(D)** Representative confocal images of cerebral cortex, choroid plexus, dentate gyrus and spinal cord in CD19-Tomato mice. B cells are not present in the CNS parenchyma (scale bar=50μm). **(E)** Representative confocal images of B cells in the leptomeninges, showing both extravascular B cells (white arrowhead) and intravascular B cells (yellow arrowhead) (scale bar=50μm).

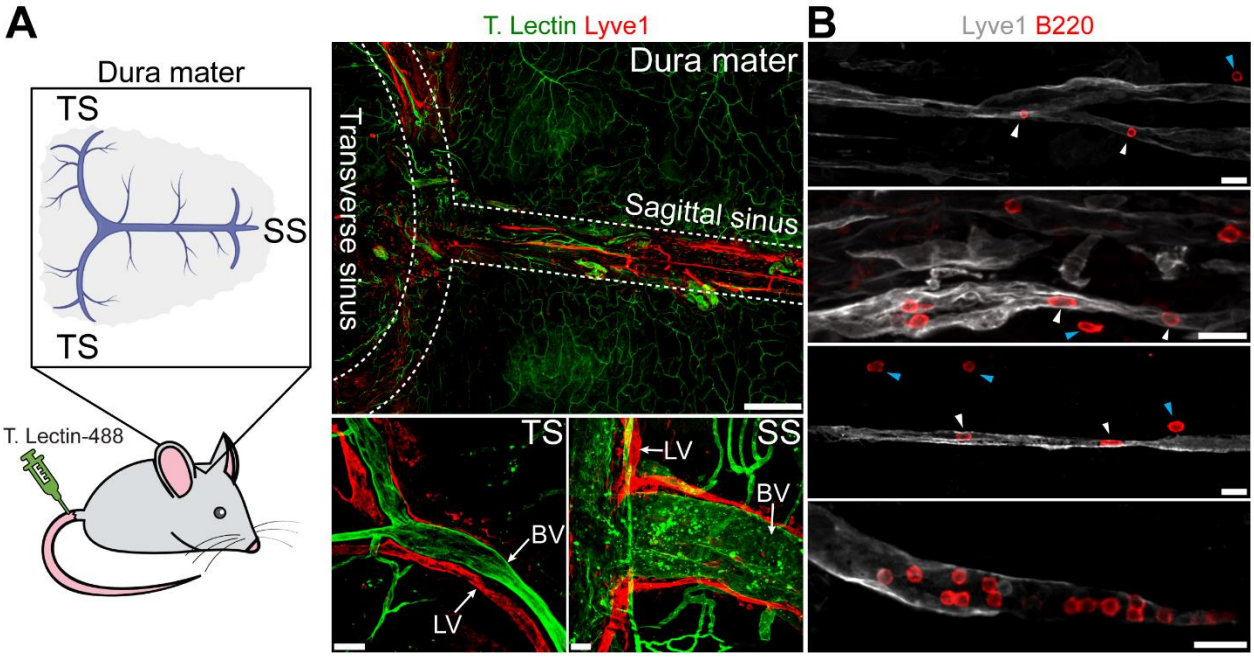

Fig. S2. Meningeal B cell trafficking through the dura lymphatics. (A) Confocal imaging of dura mater (SS: sagittal sinus; TS: transverse sinus) under Tomato-lectin (blood vessels) and Lyve-1 (lymphatic vessels) staining (low magnification image scale bar=500μm; high magnification image scale bar=50μm). **(B)** Representative confocal image of dura mater stained for Lyve-1 and B220. B cells were localized both within (white arrowhead) and outside (blue arrowhead) the lymphatic vessels (scale bar=20μm).

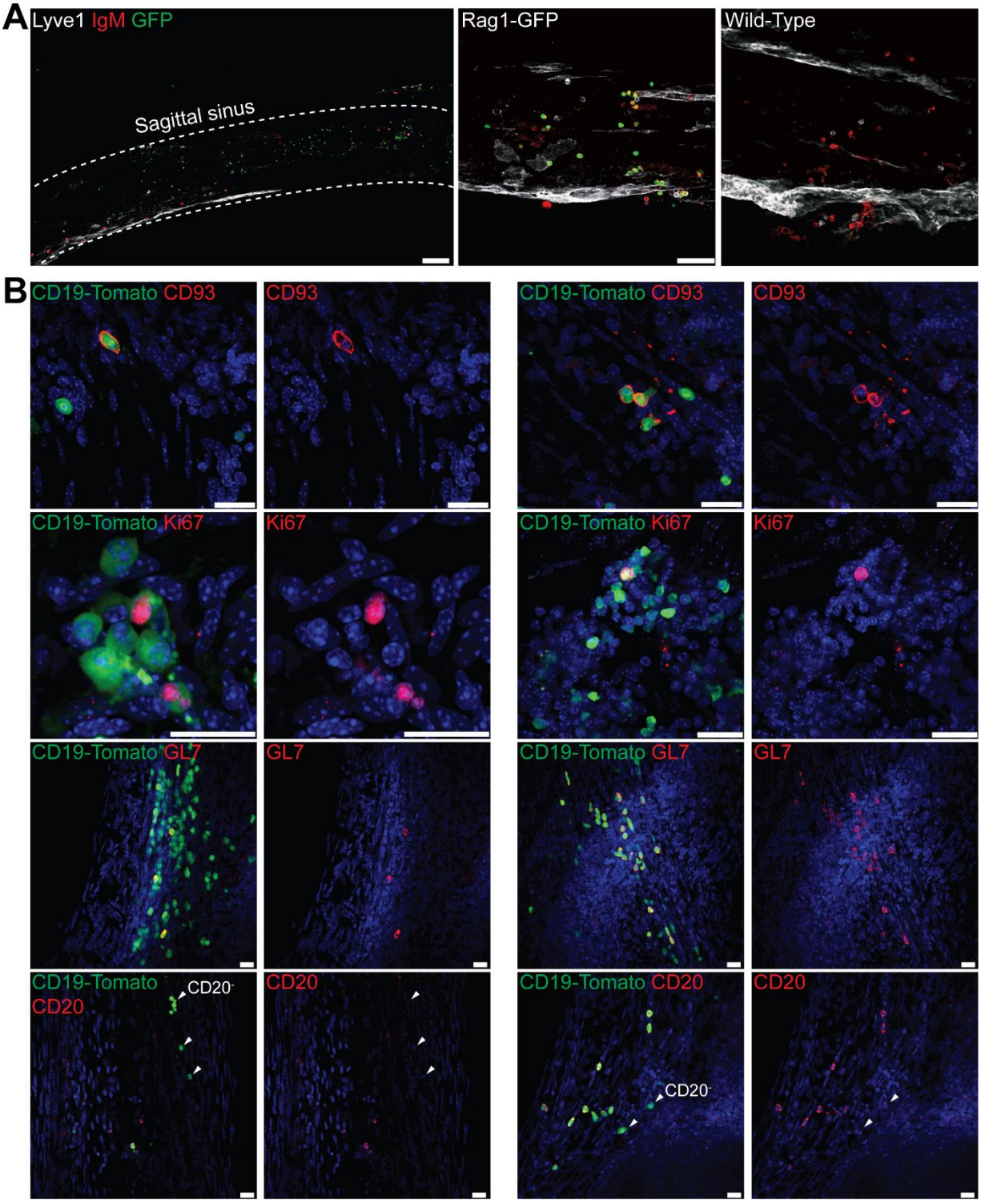

Fig. S3. Imaging of immature B cells in dura mater. (A) Representative confocal image of GFP^+ B cells in the sagittal sinus of *Rag1-GFP* mice (representative of n=5 mice; low magnification image scale bar=100μm; high magnification image scale bar=50μm). **(B)** Representative confocal images of dura B cells stained for immature B cell markers (CD93, Ki67, and GL7) and mature B cell marker (CD20) in CD19-tomato mice. White arrowheads indicate $CD20^-$ B cells (each column displays a representative image from two different mice; scale bar=20μm).

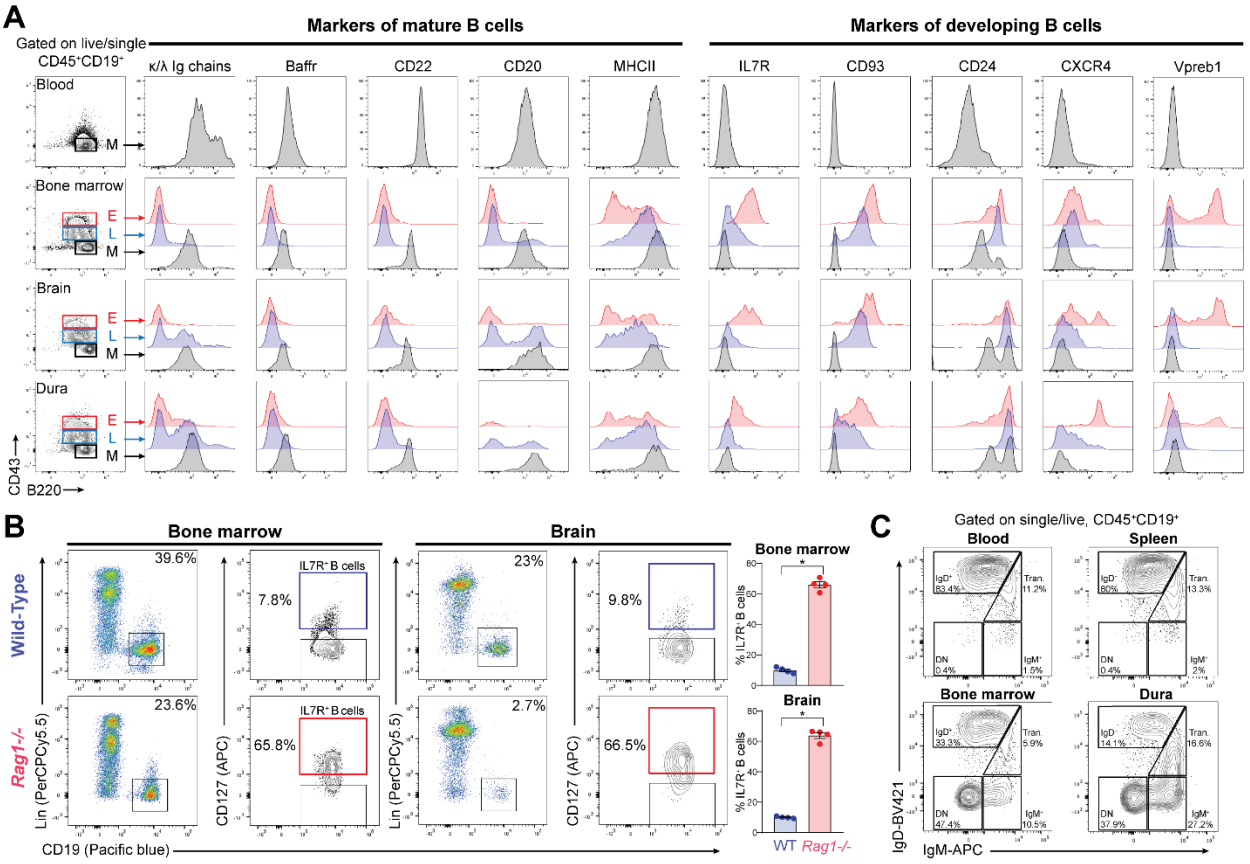

Fig. S4. Phenotypic characterization of meningeal B cells. (A) Flow cytometry analysis of blood, bone marrow (BM), brain and dura B cells. B cells were gated on $CD45^{+}CD19^{+}$ and Lineage (CD3, CD11b, F4/80 and Gr-1) negative and were further divided into early ($B220^{lo}CD43^{hi}$), late ($B220^{lo}CD43^{lo}$) and mature ($B220^{hi}CD43^{-}$) stages. Histograms show the staining intensity of mature B cell markers and developing B cell markers in the three subsets (data generated from a single experiment). **(B)** Flow cytometry analysis of IL-$7R^{+}$ (CD127) B cells in BM and brain from C57BL/6 and $Rag1^{-/-}$ mice (mean ± SEM; n=4 mice per group; Mann Whitney *U* test **P*<0.05; data generated from a single experiment). **(C)** Flow cytometry analysis of IgD and IgM expression in B cells derived from blood, spleen, BM and dura (representative of n=3 mice; data generated from a single experiment).

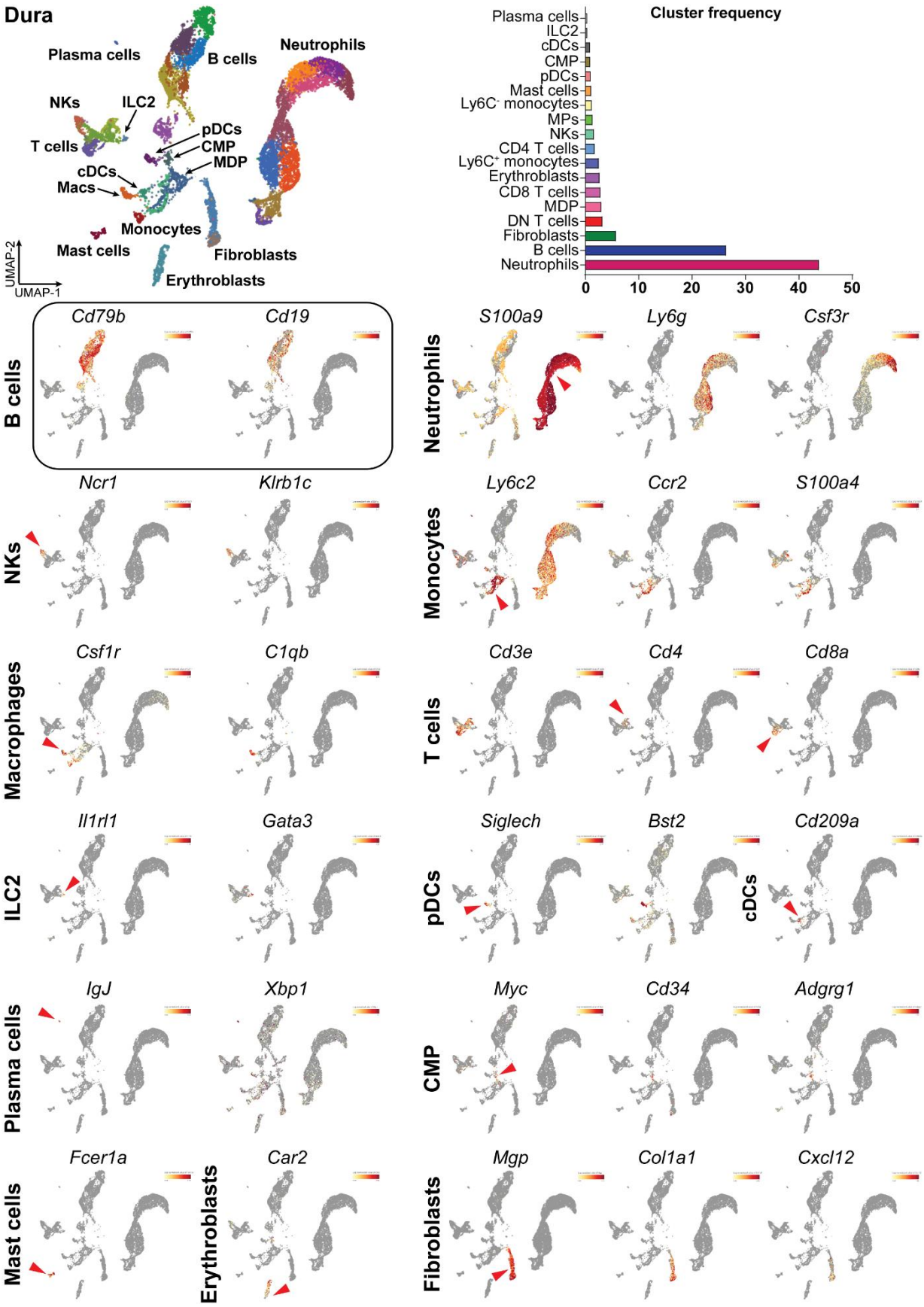
Dura
Plasma cells
B cells
Neutrophils
NKs
ILC2
T cells
pDCs
CMP
MDP
cDCs
Macs
Monocytes
Mast cells
Fibroblasts
Erythroblasts
UMAP-2
UMAP-1
Cluster frequency
Plasma cells
ILC2
cDCs
CMP
pDCs
Mast cells
Ly6C- monocytes
MPs
NKs
CD4 T cells
Ly6C+ monocytes
Erythroblasts
CD8 T cells
MDP
DN T cells
Fibroblasts
B cells
Neutrophils
0
10
20
30
40
50
B cells
Cd79b
Cd19
Neutrophils
S100a9
Ly6g
Csf3r
NKs
Ncr1
Klrb1c
Monocytes
Ly6c2
Ccr2
S100a4
Macrophages
Csf1r
C1qb
T cells
Cd3e
Cd4
Cd8a
ILC2
Il1rl1
Gata3
pDCs
Siglech
Bst2
cDCs
Cd209a
Plasma cells
IgJ
Xbp1
CMP
Myc
Cd34
Adgrg1
Mast cells
Fcer1a
Erythroblasts
Car2
Fibroblasts
Mgp
Col1a1
Cxcl12

Fig. S5. scRNA-seq analysis of dura cells. Top left, UMAP of total 12,351 cells from dura. Cells were colored by cell type and annotated with inferred cluster identities. Top right, frequency of cell types identified in dura. Bottom, expression of lineage specific genes in the corresponding cell types (n=3 mice; data generated from a single experiment).

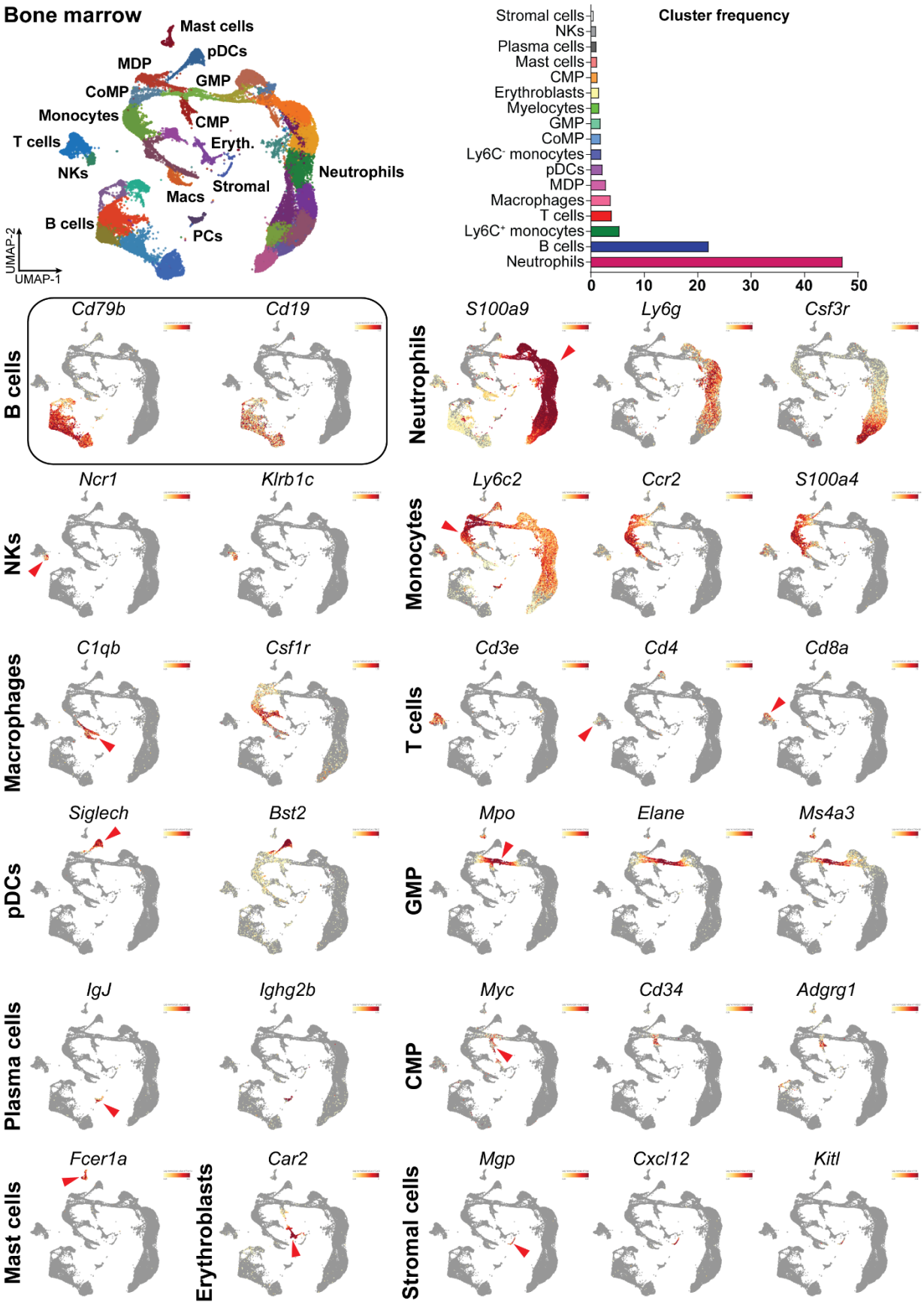
Bone marrow
Mast cells
pDCs
MDP
GMP
CoMP
Monocytes
CMP
T cells
Eryth.
NKs
Neutrophils
Stromal
Macs
B cells
PCs
UMAP-2
UMAP-1
Cluster frequency
Stromal cells
NKs
Plasma cells
Mast cells
CMP
Erythroblasts
Myelocytes
GMP
CoMP
Ly6C- monocytes
pDCs
MDP
Macrophages
T cells
Ly6C+ monocytes
B cells
Neutrophils
0
10
20
30
40
50
B cells
Cd79b
Cd19
Neutrophils
S100a9
Ly6g
Csf3r
NKs
Ncr1
Klrb1c
Monocytes
Ly6c2
Ccr2
S100a4
Macrophages
C1qb
Csf1r
T cells
Cd3e
Cd4
Cd8a
pDCs
Siglech
Bst2
GMP
Mpo
Elane
Ms4a3
Plasma cells
IgJ
Ighg2b
CMP
Myc
Cd34
Adgrg1
Mast cells
Fcer1a
Erythroblasts
Car2
Stromal cells
Mgp
Cxcl12
Kitl

Fig. S6. scRNA-seq analysis of BM cells. Top left, UMAP of total 36,452 cells from BM. Cells were colored by cell type and annotated with inferred cluster identities. Top right, frequency of cell types identified in BM. Bottom, expression of lineage specific genes in the corresponding cell types (n=3 mice; data generated from a single experiment).

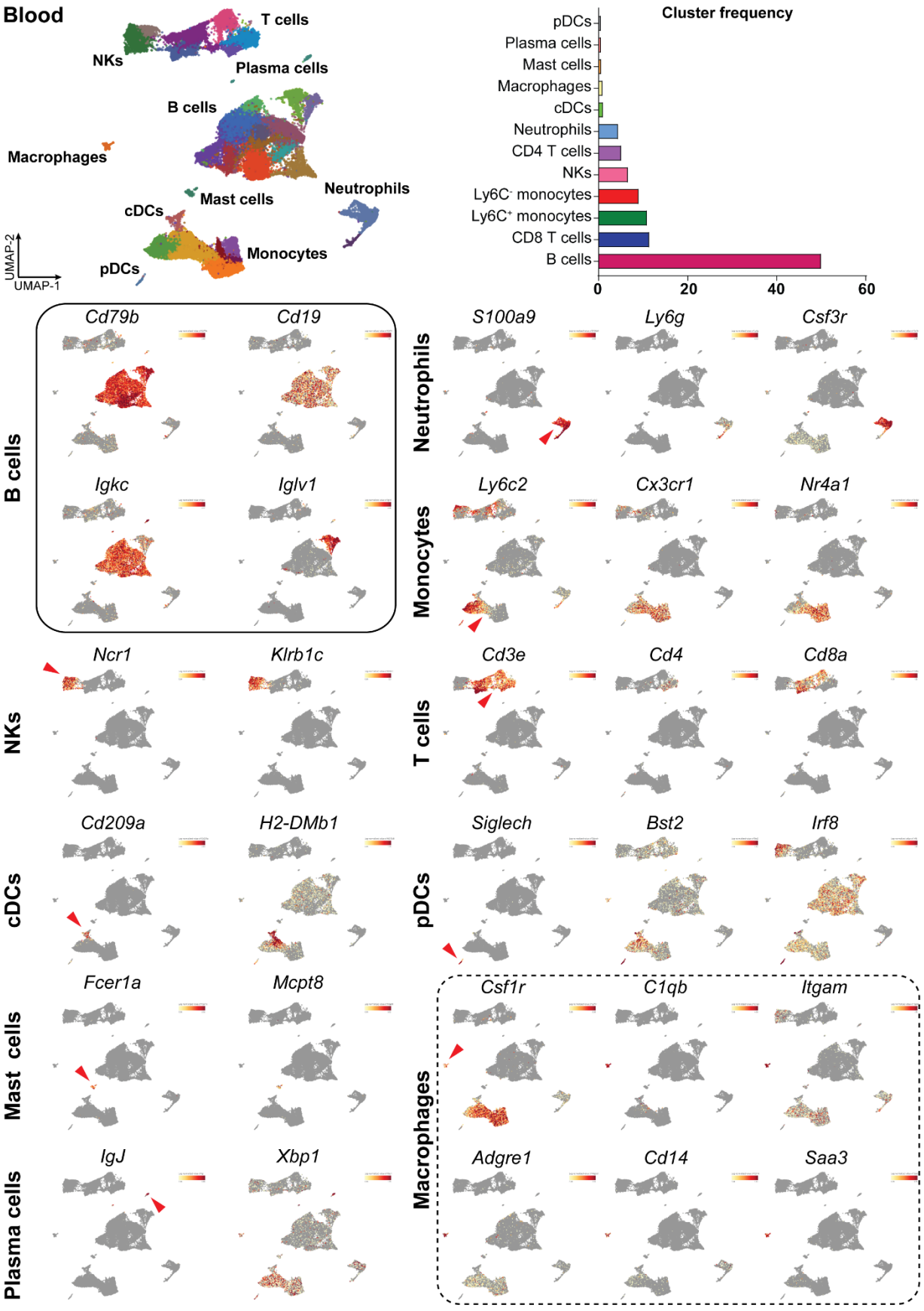
Blood
T cells
NKs
Plasma cells
B cells
Macrophages
Mast cells
Neutrophils
cDCs
Monocytes
pDCs
UMAP-2
UMAP-1
Cluster frequency
pDCs
Plasma cells
Mast cells
Macrophages
cDCs
Neutrophils
CD4 T cells
NKs
Ly6C⁻ monocytes
Ly6C⁺ monocytes
CD8 T cells
B cells
0
20
40
60
B cells
Cd79b
Cd19
Igkc
Iglv1
Neutrophils
S100a9
Ly6g
Csf3r
Monocytes
Ly6c2
Cx3cr1
Nr4a1
NKs
Ncr1
Klrb1c
T cells
Cd3e
Cd4
Cd8a
cDCs
Cd209a
H2-DMb1
pDCs
Siglech
Bst2
Irf8
Mast cells
Fcer1a
Mcpt8
Macrophages
Csf1r
C1qb
Itgam
Plasma cells
IgJ
Xbp1
Adgre1
Cd14
Saa3

Fig. S7. scRNA-seq analysis of blood cells. Top left, UMAP of total 42,370 cells from blood. Cells were colored by cell type and annotated with inferred cluster identities. Top right, frequency of cell types identified in blood. Bottom, expression of lineage specific genes in the corresponding cell types (n=3 mice; data generated from a single experiment).

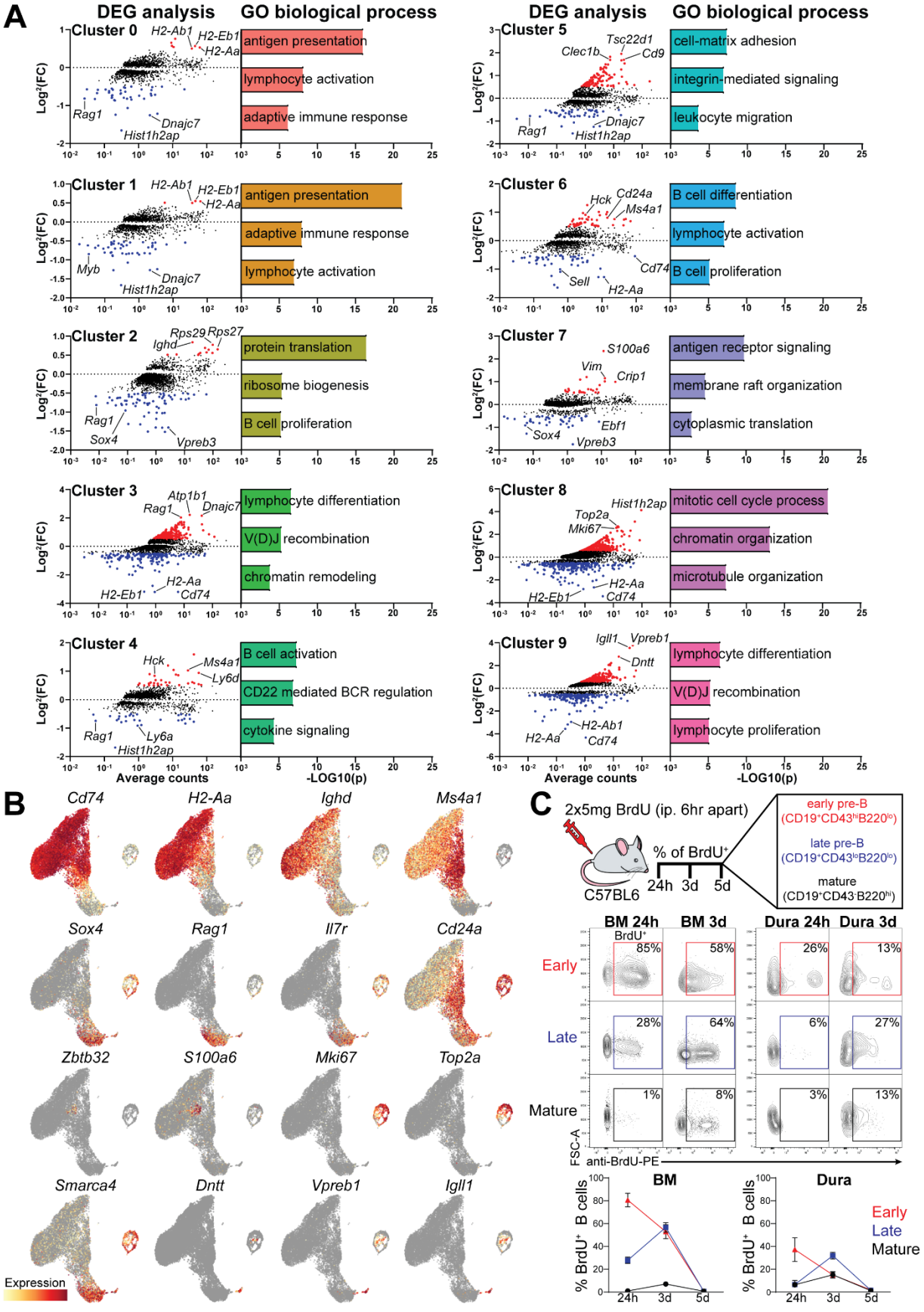
A
DEG analysis
GO biological process
Cluster 0
H2-Ab1
H2-Eb1
H2-Aa
Rag1
Dnajc7
Hist1h2ap
antigen presentation
lymphocyte activation
adaptive immune response
Cluster 1
Myb
antigen presentation
adaptive immune response
lymphocyte activation
Cluster 2
Rps29
Rps27
Ighd
Sox4
Vpreb3
protein translation
ribosome biogenesis
B cell proliferation
Cluster 3
Atp1b1
lymphocyte differentiation
V(D)J recombination
chromatin remodeling
Cluster 4
Hck
Ms4a1
Ly6d
Ly6a
B cell activation
CD22 mediated BCR regulation
cytokine signaling
Cluster 5
Tsc22d1
Clec1b
Cd9
cell-matrix adhesion
integrin-mediated signaling
leukocyte migration
Cluster 6
Cd24a
Cd74
Sell
B cell differentiation
lymphocyte activation
B cell proliferation
Cluster 7
S100a6
Vim
Crip1
Ebf1
antigen receptor signaling
membrane raft organization
cytoplasmic translation
Cluster 8
Hist1h2ap
Top2a
Mki67
mitotic cell cycle process
chromatin organization
microtubule organization
Cluster 9
Igll1
Vpreb1
Dntt
lymphocyte differentiation
V(D)J recombination
lymphocyte proliferation
Log2(FC)
Average counts
-LOG10(p)
B
Cd74
H2-Aa
Ighd
Ms4a1
Sox4
Rag1
Il7r
Cd24a
Zbtb32
S100a6
Mki67
Top2a
Smarca4
Dntt
Vpreb1
Igll1
Expression
C
2x5mg BrdU (ip. 6hr apart)
% of BrdU+
24h 3d 5d
C57BL6
early pre-B
(CD19+CD43hiB220lo)
late pre-B
(CD19+CD43loB220lo)
mature
(CD19+CD43-B220hi)
BM 24h
BM 3d
Dura 24h
Dura 3d
BrdU+
Early
Late
Mature
85%
58%
26%
13%
28%
64%
6%
27%
1%
8%
3%
13%
FSC-A
anti-BrdU-PE
BM
Dura
% BrdU+ B cells
Early
Late
Mature

Fig. S8. Transcriptional signature of the identified B cell clusters. (A) Differential gene expression analysis (cluster vs total; cutoff=$log_2FC>0.5$) and enriched biological processes in each B cell cluster (from C0 to C9). **(B)** Expression of marker genes differentially expressed during B cell development. **(C)** BrdU pulse-chase labeling of proliferating B cells in BM and dura. BrdU incorporation was assessed at three time-points (24hrs, 3 days and 5 days post-injection) in early ($CD19^+CD43^{hi}B220^{lo}$), late ($CD19^+CD43^{lo}B220^{lo}$) and mature ($CD19^+CD43^-B220^{hi}$) B cell. Dynamic distribution of $BrdU^+$ B cells among the three subsets is shown in the bottom panel (n=3 mice per time-point; data generated from two independent experiments).

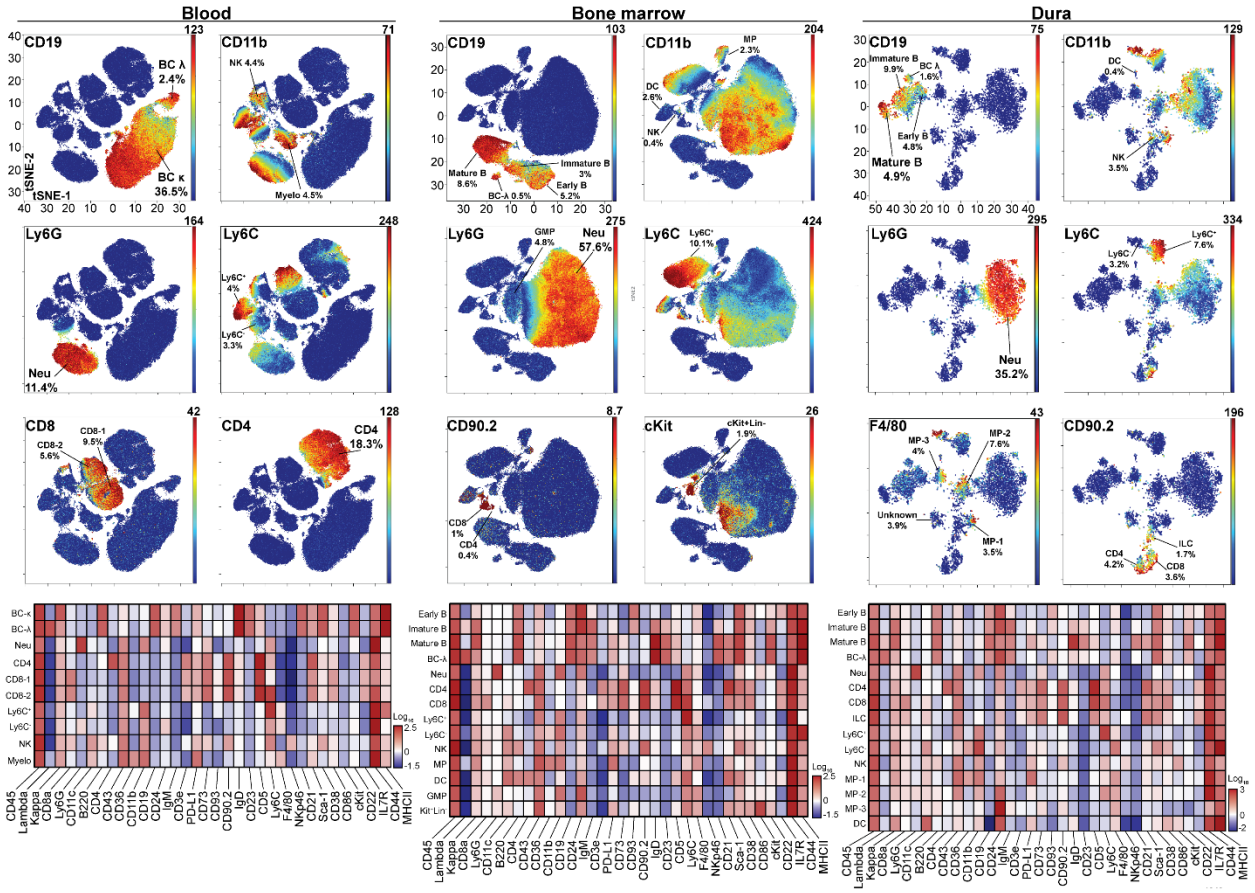

Fig. S9. High-throughput characterization of immune cells from blood, BM, and dura based on CyTOF analysis. Upper panels: major immune populations in blood, bone marrow, and dura displayed by tSNE. Bottom panels: heatmap showing the surface marker repertoire for each individual population (n=3 mice; data generated from a single experiment).

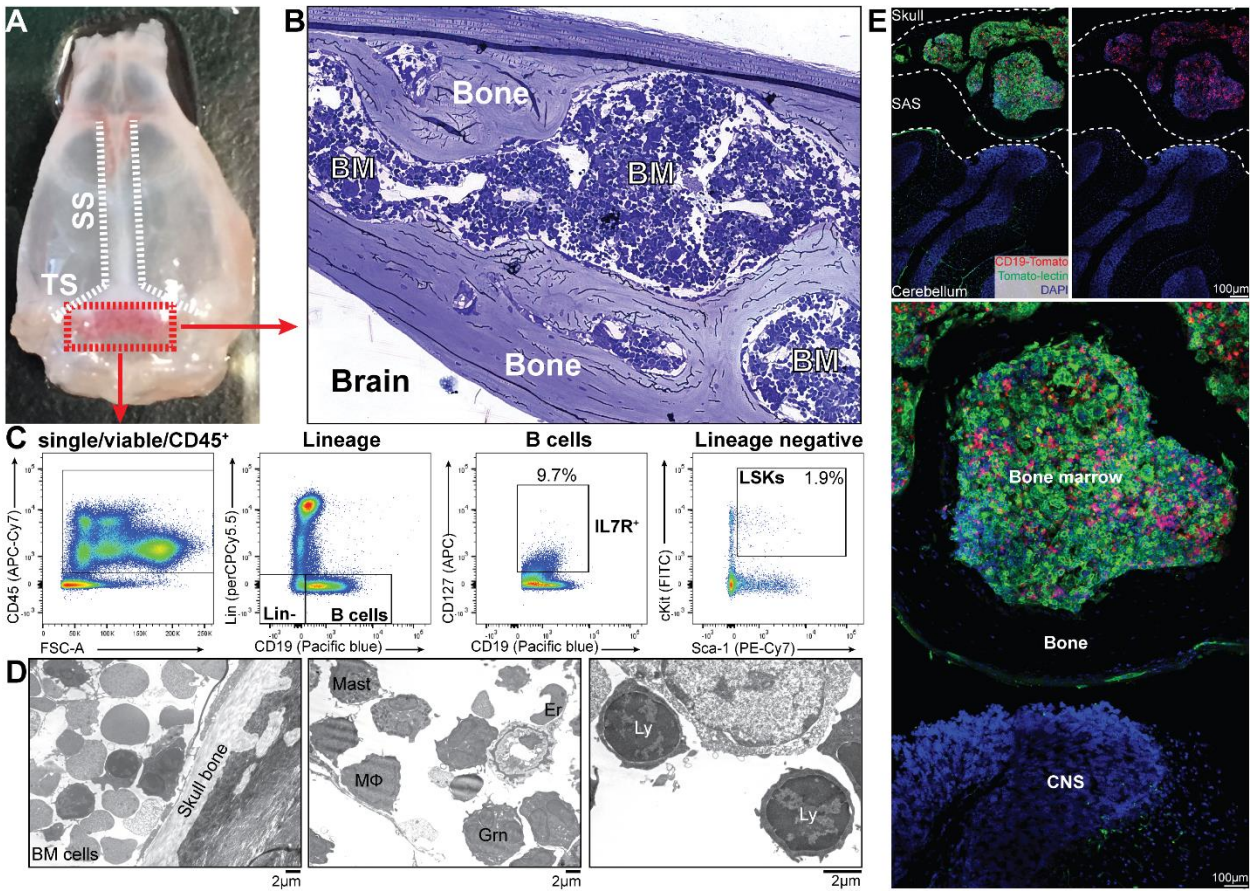

Fig. S10. The hematopoietic niche in the calvaria. (A) Image of the region enriched of BM cells in the mouse skull (red box). **(B)** Brightfield image under toluidine blue staining of the calvarial bone marrow. **(C)** FACS analysis of the calvarial $CD45^+$ BM cells. Both $IL7R^+$ B cells and $Lin^-Sca1^+Kit^+$ stem cells were found. **(D)** EM micrographs of the calvarial BM, showing both myeloid cells (bona-fide macrophages, granulocytes, mast cells and erythrocytes) and lymphoid cells (bona-fide lymphocytes). **(E)** Confocal images of cranial sagittal section from a CD19-Tomato mouse stained with Tomato-lectin. Whereas no B cells are visible in the brain parenchyma, abundant B cells are present within the calvarial BM.

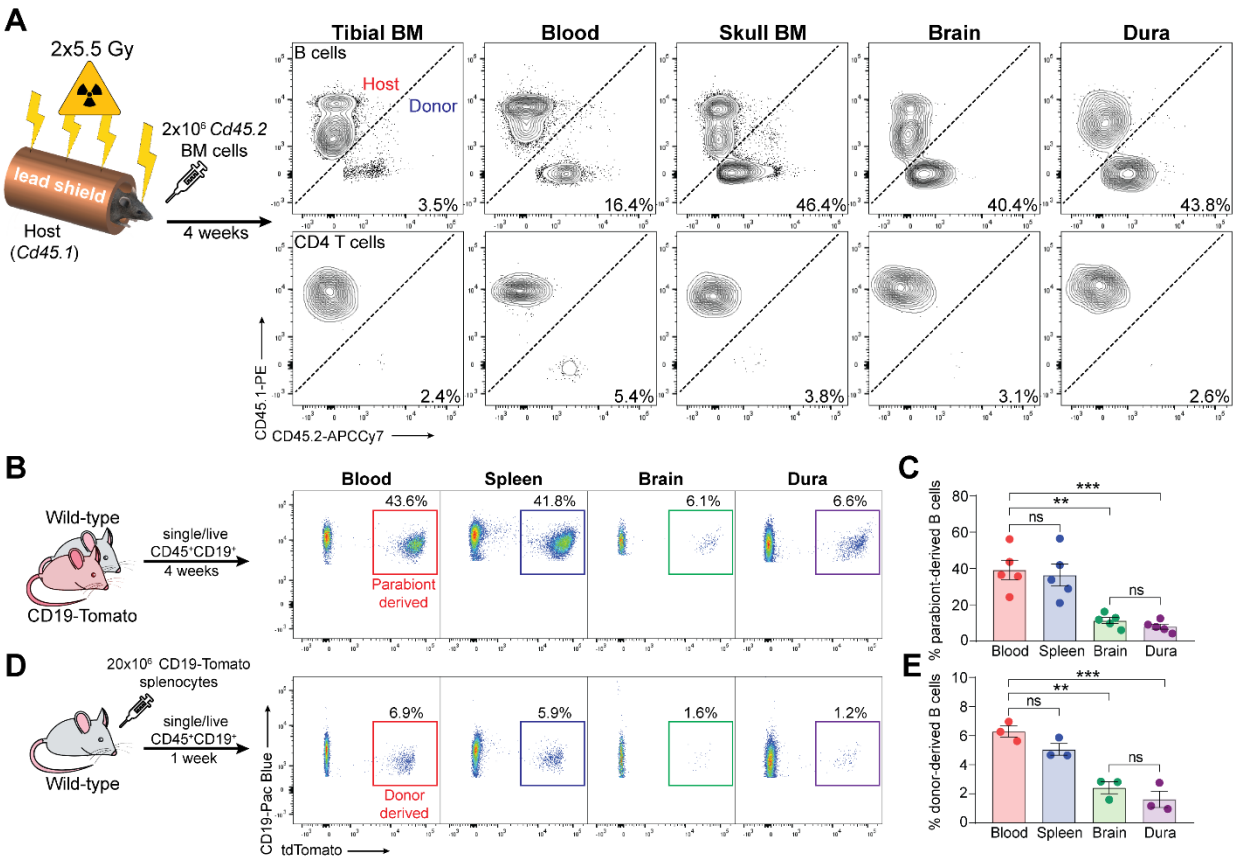

Fig. S11. Meningeal B cells derive from the calvaria. (A) Flow cytometry analysis of donor-derived (CD45.2$^+$) and host-derived (CD45.1$^+$) B cells and CD4 T cells in different compartments of head-reconstituted mice (representative of two mice; data generated from a single experiment). **(B)** Four weeks parabiosis between wild-type C57BL/6 and CD19-Tomato mice. Flow cytometry analysis of the wild type parabiont shows the percentage of B cells chimerism in blood, spleen, brain, and dura. **(C)** Frequency of parabiont-derived B cells in the indicated tissues (mean ± SEM; n=5 mice; one-way ANOVA and Bonferroni post-hoc test ***P*<0.01, ****P*<0.001; data generated from three independent experiments). **(D)** Adoptive transfer by iv. injection of 20x10^6 CD19-Tomato splenocytes into wild-type C57BL/6 mouse. Flow cytometry analysis one week post-injection shows the percentage of donor-derived B cells in blood, spleen, brain, and dura. **(E)** Frequency of donor-derived B cells in the indicated tissues (mean ± SEM; n=3 mice; one-way ANOVA and Bonferroni post-hoc test ***P*<0.01, ****P*<0.001; data representative of two independent experiments).

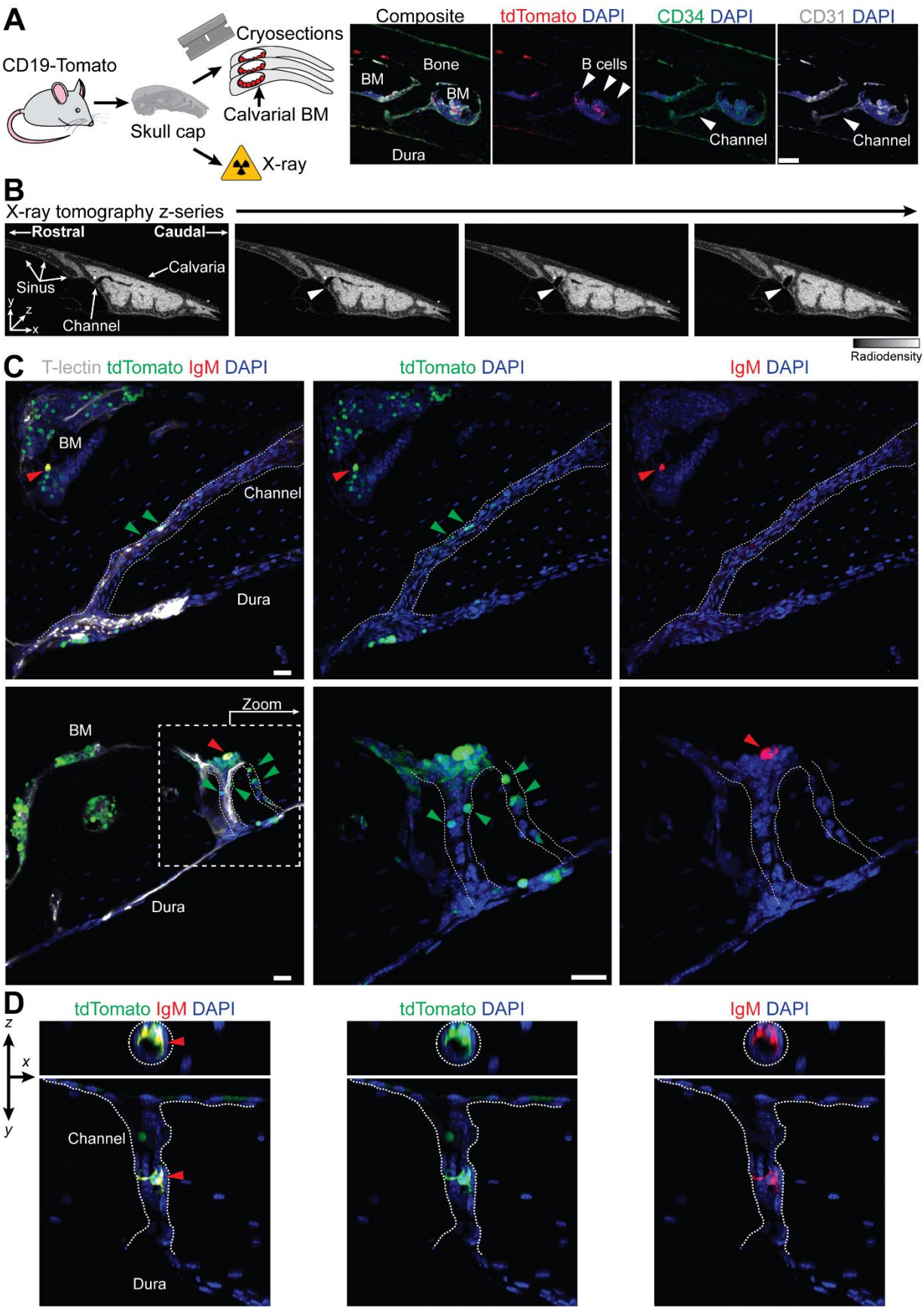
A
CD19-Tomato
Cryosections
Skull cap
Calvarial BM
X-ray
Composite
tdTomato DAPI
CD34 DAPI
CD31 DAPI
Bone
BM
BM
B cells
Dura
Channel
Channel
B
X-ray tomography z-series
Rostral
Caudal
Calvaria
Sinus
Channel
Radiodensity
C
T-lectin tdTomato IgM DAPI
tdTomato DAPI
IgM DAPI
BM
Channel
Dura
Zoom
BM
Dura
D
tdTomato IgM DAPI
tdTomato DAPI
IgM DAPI
z
x
y
Channel
Dura

Fig. S12. B cells trafficking through the skull vascular channel. (A) Left, schematic of sample preparation for skull cryosection and X-ray tomography. Right, representative confocal images of skull vascular channels (scale bar=50μm). **(B)** X-ray tomography images displayed as *z*-series showing a vascular channel opening onto the sinus (white arrowhead). **(C)** Representative confocal images of IgM^- B cells trafficking through the skull vascular channels (scale bar=20μm). **(D)** Orthogonal projection of a B cell within a vascular channel (red arrowhead).

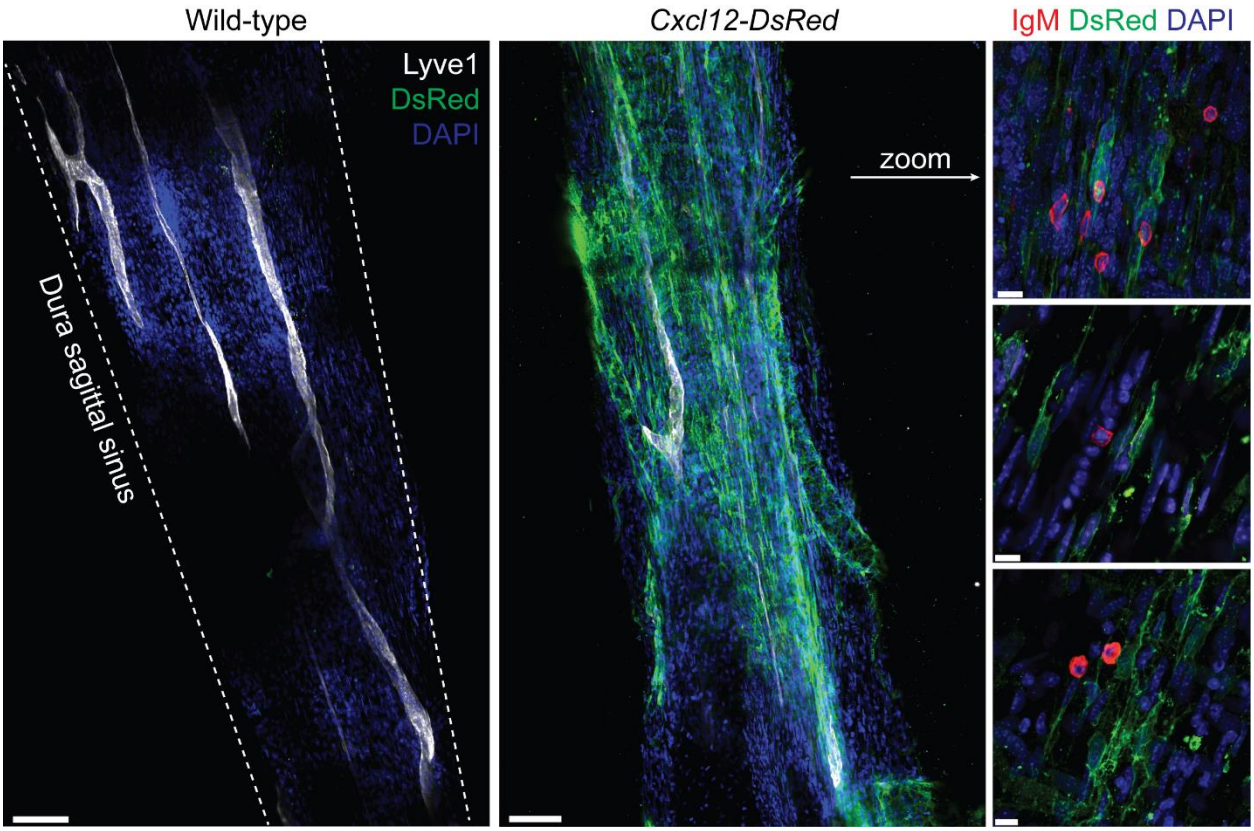

Fig. S13. *Cxcl12* expression in the sagittal sinus. Representative confocal images of dura sagittal sinus from a WT and *a Cxcl12-DsRed* reporter mouse under Lyve-1 staining. High magnification images of Cxcl12-expressing fibroblasts (scale bar=100μm) and IgM^+ B cells are shown on the right (scale bar=10μm).

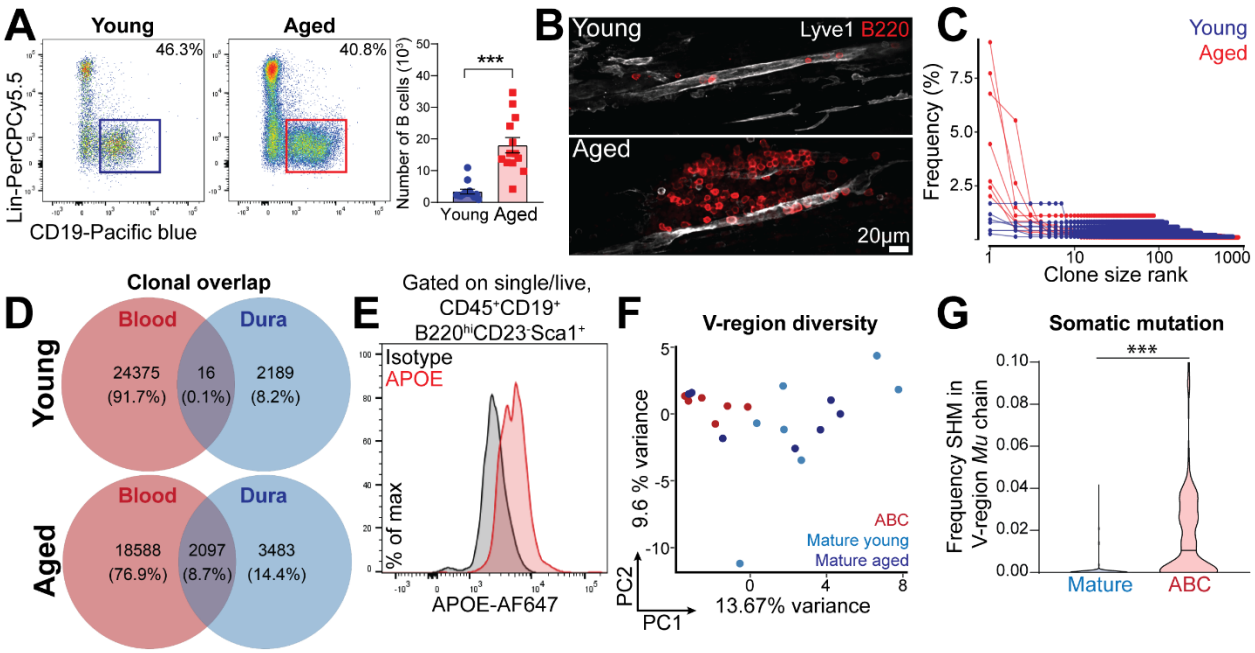

Fig. S14. Meningeal B cells during aging. (A) Flow cytometry analysis of dura B cells in young and aged mice (mean ± SEM; n=13 mice; Unpaired Student's *t* test ***P<0.001; data generated from three independent experiments). **(B)** Confocal imaging of B cells in the sagittal sinus of young and aged mice. **(C)** Frequency of B cells clones ranked by size. Each line represents an individual mouse. **(D)** Fraction of B cell clones shared between blood and dura in young and aged mice. **(E)** Flow cytometry intracellular staining of ApoE in dura ABC population (data generated from a single experiment). (**F)** Principal component analysis of V-region diversity in dura ABCs and dura mature B cells from young and aged mice. **(G)** Frequency of somatic mutations in V-region from dura mature B cells and dura ABCs expressing *Ighm* (violin plot, Mann Whitney *U* test ***P<0.001).

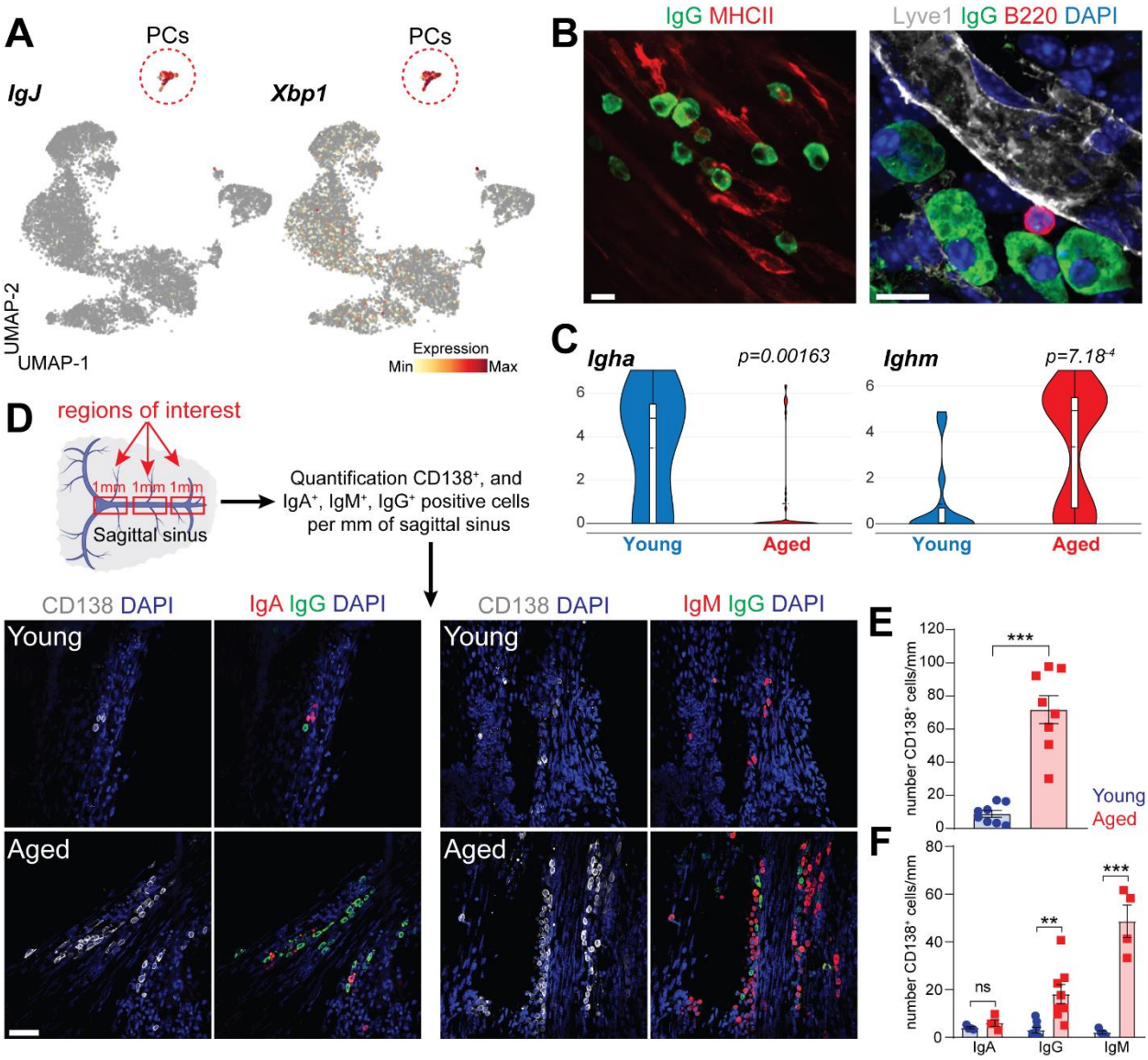

Fig. S15. IgM plasma cells accumulate in the aged dura. (A) Plasma cells cluster in dura enriched for signature genes (*IgJ* and *Xbp1*). **(B)** Representative images of dura plasma cells ($IgG^+MHC\text{-}II^-B220^-$) (scale bar=10μm). **(C)** Differential expression levels of *Igha* and *Ighm* in dura plasma cells from young and aged mice. **(D)** Dura plasma cells were imaged and quantified in young and aged mice. The cartoon indicates the approximate position of three regions of interest (y,x,z = 1000μm x 350μm x 10μm) used for imaging. Plasma cells number per mm of sagittal sinus was determined by averaging the absolute count in the three regions of interest in each mouse (scale bar=50μm). **(E)** Number of total plasma cells per mm of sagittal sinus in young and aged mice (mean ± SEM; n=8 mice; unpaired Student's *t* test ***P<0.001; data generated from two independent experiments). **(F)** Number of IgA, IgG and IgM plasma cells per mm of sagittal sinus in young and aged mice (mean ± SEM; n=4-8 mice per group; two-ways ANOVA and Bonferroni post-hoc test **P<0.01, ***P<0.001; data generated from two independent experiments).

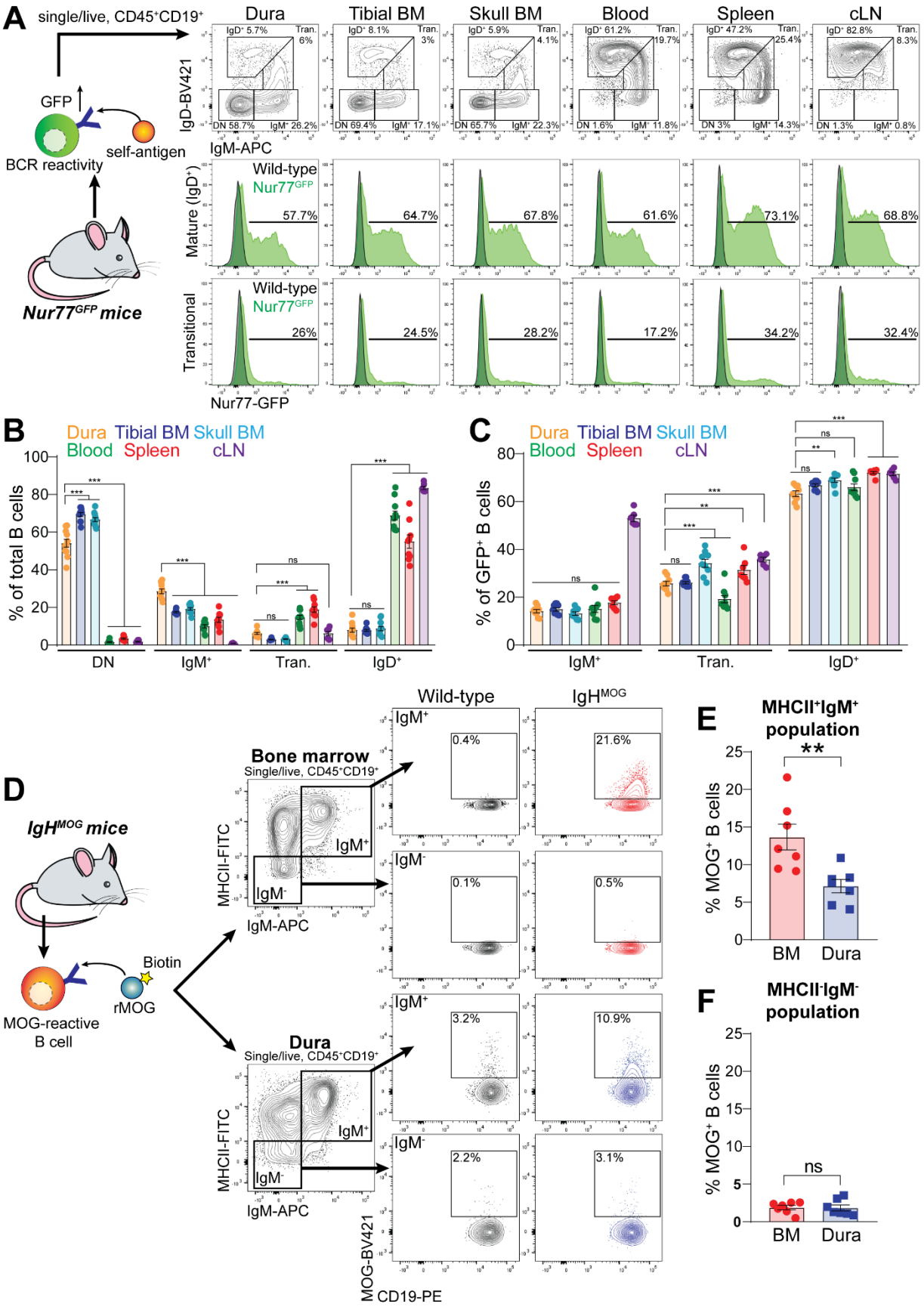
A
single/live, CD45+CD19+
GFP
self-antigen
BCR reactivity
Nur77GFP mice
Dura
Tibial BM
Skull BM
Blood
Spleen
cLN
IgD-BV421
IgM-APC
Mature (IgD+)
Transitional
Wild-type
Nur77GFP
Nur77-GFP
B
Dura Tibial BM Skull BM
Blood Spleen cLN
% of total B cells
DN
IgM+
Tran.
IgD+
C
% of GFP+ B cells
D
IgHMOG mice
Biotin
rMOG
MOG-reactive B cell
Bone marrow
Single/live, CD45+CD19+
Dura
MHCII-FITC
IgM-APC
Wild-type
IgHMOG
MOG-BV421
CD19-PE
E
MHCII+IgM+ population
% MOG+ B cells
BM
Dura
F
MHCII-IgM- population

Fig. S16. Dura B cells are equipped with functional BCRs, and MOG-specific B cells are reduced in dura compared to tibial BM. (A) Flow cytometry analysis of B cells from *Nur77*^{GFP} mice in multiple compartments: dura, tibial BM, skull BM, blood, spleen, and cervical lymph nodes (cLN). B cells were gated as: IgM/IgD double negative (DN), IgM$^+$, IgM$^+$IgD^{lo} (transitional), and IgD$^+$. Frequency of these population and percentage of GFP$^+$ cells was determined in all compartments. **(B)** Percentage of different B cell populations from all analyzed tissues (mean ± SEM; n=7-11 mice per group; two-ways ANOVA and Bonferroni post-hoc test ***P<0.001; data generated from two independent experiments). **(C)** Percentage of GFP$^+$ B cell in different populations from all analyzed tissues (mean ± SEM; n=6-9 mice per group; two-ways ANOVA and Bonferroni post-hoc test **P<0.01, ***P<0.001; data generated from two independent experiments). **(D)** Flow cytometry analysis of B cells from *IGH*^{MOG} mice in dura and tibial BM. B cells were gated as: MHC-II$^+$IgM$^+$ and MHC-II$^-$IgM$^-$. Percentage of MOG-binding B cells was determined each population. Wild-type mice served as negative control. **(E)** Quantification of MOG-specific B cells in dura and tibial BM MHC-II$^+$IgM$^+$ B cells (mean ± SEM; n=7 mice; unpaired Student's *t* test **P*<0.01;* data generated from two independent experiments). **(F)** Quantification of MOG-specific B cells in dura and tibial BM MHC-II$^-$IgM$^-$ B cells (mean ± SEM; n=7 mice; unpaired Student's *t* test; data generated from two independent experiments).

Movie S1
Two photon in vivo imaging of meningeal B cells.

Movie S2
X-ray tomography of the intact mouse skull.

Table S1
Transcriptional signature for each B cell cluster identified by scRNA-seq.

Table S2
Surface markers expression for each B cell cluster identified by CyTOF.

Table S3
Transcriptional signature of dura ABCs identified by scRNA-seq.

Table S4
Complete antibody list used for flow cytometry, immunofluorescence and CyTOF staining.